

On the Design and Optimization of the Shielded-Pair Transmission Line

GLENN S. SMITH, MEMBER, IEEE, AND JOHN D. NORDGÅRD, MEMBER, IEEE

Abstract—The electrical parameters of the shielded-pair transmission line are computed using a truncated harmonic expansion for the surface charge density on the conductors. The formulation includes the proximity effect due to the close spacing of the conductors. Parametric curves are given for the capacitance, resistance, and attenuation per-unit length, and the characteristic impedance of the line. Both the balanced and the longitudinal modes of propagation are considered and the dimensions for a line with minimum attenuation are determined for each mode. Capacitances measured on model transmission lines are shown to be in good agreement with the theory.

I. INTRODUCTION

SEVERAL DIFFERENT methods for computing the electrical characteristics of multiconductor transmission systems have been presented in the literature. These structures have been analyzed using physical approximations, such as the replacement of the conductors by image line charges [1]–[3], conformal mapping [4], variational principles [5], and matrix methods that involve truncating an infinite series of harmonic terms that represent the surface charge or current on the conductors (often referred to generically as the method of moments) [6]–[7]. When used with a modern computer, the last approach offers the advantage that any reasonable degree of accuracy for the parameters, such as the capacitances per-unit length, can be obtained by retaining a sufficient number of terms in the series. The papers that cover this material generally have presented numerical results for a few specific cases, but no systematic parametric studies that can be used for design purposes.

The parameters that characterize the shielded-pair transmission line are of particular interest since this structure is often used in practice, e.g., as a shielded balanced transmission line in telephonic communication, and in directional couplers, transformers and filters at radio frequencies (UHF). Several approximate formulas were developed for the capacitances per-unit length of this line during the early period of its use [18]–[20]. Craggs and Tranter appear to be the first to have developed the matrix method for this geometry; however, at that time, the application of the method was severely restricted by the limited computational facilities [6], [7]. Recently the matrix method has been used with modern computers to produce highly accurate values of the capacitances per-

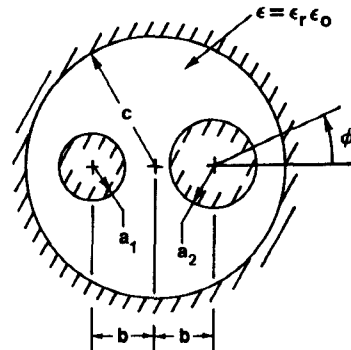


Fig. 1. Geometry of shielded-pair transmission line.

unit length of this structure [8], [12]–[16]. In this paper, expressions for the other parameters that characterize the structure are also determined, i.e., resistance and attenuation per-unit length and the characteristic impedance. Accurate parametric representations of these characteristics are presented in graphical form. These graphs are useful in the design and the optimization of shielded-pair transmission lines. Capacitances measured on models of these transmission lines are compared with the theory.

The geometry of the shielded-pair line is shown in Fig. 1. The radius of the shield is c , the half-spacing between the two conductors is b , and the dielectric in the line has the relative permittivity $\epsilon_r = \epsilon/\epsilon_0$. The two inner conductors of the line may have different radii a_1 and a_2 , but their axes and the axis of the shield are assumed to be coplanar and, of course, parallel. The propagation of transverse electromagnetic (TEM) waves on the shielded-pair line constructed from perfect conductors is completely characterized by the solution of the electrostatic problem on a cross section. In the electrostatic analysis, the surface charge density η_i on the i th conductor is written as a truncated Fourier series with the form

$$\eta_i(\phi) = \sum_{n=0}^m \xi_{in} \cos(n\phi), \quad i = 1, 2, 3 \quad (1)$$

where m is the number of terms retained in the series. Note that the series also would include terms of the form $\sin(n\phi)$ if the axes of the three conductors were not coplanar. The total charge per-unit length on the i th conductor is $\lambda_i = 2\pi a_i \xi_{i0}$, where a_i is the radius of the conductor, for the shield $a_3 = c$. The linear relations between the charge coefficients ξ_{in} , and the electrostatic

Manuscript received January 9, 1980; revised March 18, 1980.
The authors are with the School of Electrical Engineering, Georgia Institute of Technology, Atlanta, GA.

potentials Φ_i on the inner conductors of the line are, in matrix form

$$\begin{bmatrix} c_{11} & c_{12} & \cdot & \cdot & \cdot \\ c_{21} & c_{22} & \cdot & \cdot & \cdot \\ \vdots & \vdots & \Gamma & & \end{bmatrix} \begin{bmatrix} \Phi_1 \\ \Phi_2 \\ 0 \\ \vdots \\ 0 \end{bmatrix} = \begin{bmatrix} \lambda_1 \\ \lambda_2 \\ \lambda_3 \\ \vdots \\ 2\pi a_1 \xi_{11} \\ 2\pi a_2 \xi_{21} \\ 2\pi c \xi_{31} \\ \vdots \\ 2\pi a_1 \xi_{1m} \\ 2\pi a_2 \xi_{2m} \\ 2\pi c \xi_{3m} \end{bmatrix} \quad (2)$$

where the potential on the shield is set equal to zero. Once the coefficients in the matrix Γ are obtained, by the method described in [12], all of the charge coefficients ξ_{in} can be determined for any excitation, i.e., any specified set of potentials Φ_1 and Φ_2 . When only the relations between the total charges per-unit length λ_i and the potentials Φ_i are of interest, only the four coefficients c_{11} , c_{12} , c_{21} , and c_{22} in the upper left-hand corner of the Γ matrix are needed. The coefficient c_{11} (c_{22}) is the ratio λ_1/Φ_1 (λ_2/Φ_2) when conductor 2 (1) is at the same potential as the shield. Note that $c_{11} = c_{22}$ when $a_1 = a_2$. The coefficient c_{12} (c_{21}) is the ratio λ_1/Φ_2 (λ_2/Φ_1) when conductor 1 (2) is at the same potential as the shield. The equality $c_{12} = c_{21}$ always holds. The terms c_{11} and c_{22} are often referred to as coefficients of capacitance per-unit length, and c_{12} and c_{21} as coefficients of induction per-unit length [21]. All of the other capacitances per-unit length that are used to characterize the structure can be computed from c_{11} , c_{22} and c_{12} . For example,

- 1) the capacitance (to ground) of one of the conductors when both conductors are at the same potential with respect to the shield (even mode of excitation)

$$c_{ge1} = c_{11} + c_{12} \quad (3)$$

$$c_{ge2} = c_{22} + c_{12} \quad (4)$$

- 2) the (mutual) capacitance between the conductors when they are at potentials that are equal in amplitude, but opposite in phase with respect to the shield (odd mode of excitation)

$$c_m = \frac{c_{11}c_{22} - c_{12}^2}{c_{11} + c_{22} + 2c_{12}}. \quad (5)$$

II. PARAMETERS FOR SYMMETRICAL SHIELDED-PAIR LINE

A case of practical interest is when the conductors 1 and 2 have the same radius ($a_1 = a_2$) and are symmetrically located within the shield. Two modes or methods of excitation are then defined, the *balanced* (odd) excitation where the conductors, 1 and 2, are at potentials that are equal in amplitude, but opposite in phase with respect to

the shield, and the *longitudinal* (even) excitation where the conductors, 1 and 2, are at the same potential with respect to the shield. The conventional transmission-line parameters are easily determined for either method of excitation once the coefficients for the charge density, ξ_{in} in (1), are known. It is convenient to define the following dimensionless transmission line parameters.

Normalized Capacitance Per-Unit Length

$$\bar{c} = \tilde{c}/\epsilon \quad (6)$$

where ϵ is the permittivity of the material filling the transmission line. The capacitance per-unit length \bar{c} is c_m for the balanced case and $2c_{ge}$ for the longitudinal case.

Normalized Characteristic Impedance

$$\bar{Z}_c = Z_c/\xi = 1/\bar{c} \quad (7)$$

where $\xi = \sqrt{\mu_0/\epsilon}$ is the wave impedance of the medium surrounding the conductors.

Normalized Resistance Per-Unit Length

At high frequencies the current in the conductors is contained in a thin layer near the surface (skin effect) and can be approximated by an axial surface current density

$$\vec{K}_{zi}(\phi) = \hat{z} \sum_{n=0}^m \xi_{in} \cos(n\phi). \quad (8)$$

The coefficient ξ_{in} in the series (8) can be obtained from those for the charge density ξ_{in} using the equation of continuity, viz.,

$$\xi_{in} = \frac{c_0}{\sqrt{\epsilon_r}} \xi_{in} \quad (9)$$

where c_0 is the speed of light in a vacuum. An approximate expression for the time-average power p_i dissipated per-unit length of conductor is obtained from the surface current and the surface resistance R_m

$$p_i = R_m \pi a_i \left(|\xi_{i0}|^2 + \frac{1}{2} \sum_{n=1}^m |\xi_{in}|^2 \right) \quad (10)$$

where

$$a_1 = a_2 = a \quad a_3 = c. \quad (11)$$

At high frequencies the surface resistance is

$$R_m \approx \sqrt{\omega \mu_0 / 2\sigma} \quad (12)$$

where σ is the conductivity of the metal. The high-frequency resistance per-unit length of the transmission line is

$$r = 2 \sum_{i=1}^3 p_i / I_0^2 \quad (13)$$

where I_0 is the average current in one of the inner conductors for the balanced case ($I_0 = 2\pi a \xi_{10}$), and twice the average current in one of the inner conductors for the longitudinal case ($I_0 = 4\pi a \xi_{10}$). After combining (9), (10), and (13), the normalized resistance per-unit length of the transmission line obtains

$$\bar{r} = \frac{2\pi c r}{R_m} = \left(\frac{c}{a} \right)^2 \sum_{i=1}^3 \left\{ \frac{a_i}{c} \left[|\bar{\xi}_{i0}|^2 + \frac{1}{2} \sum_{n=1}^m |\bar{\xi}_{in}|^2 \right] \right\} \quad (14)$$

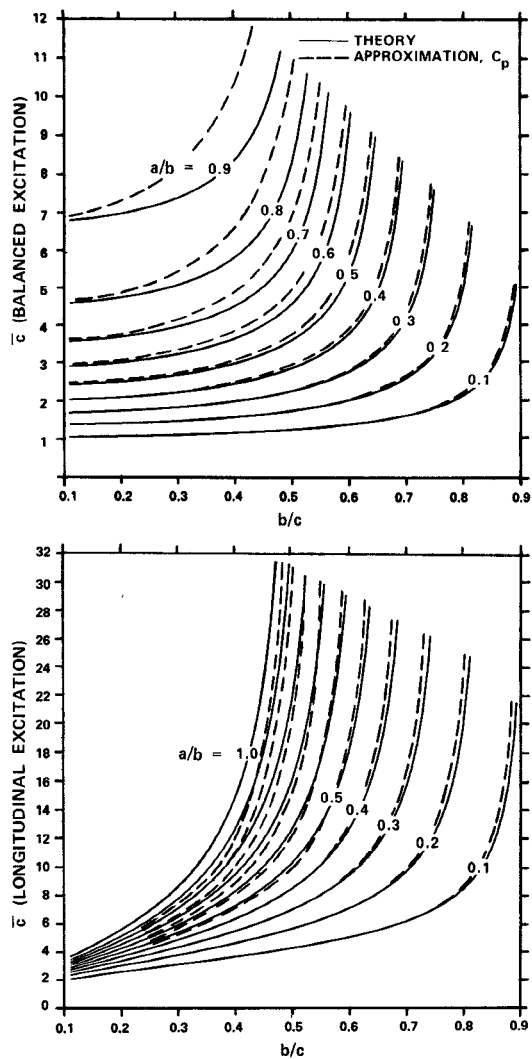


Fig. 2. Normalized capacitance per-unit length for balanced and longitudinal excitations versus separation of conductors with radius of conductor as parameter.

where

$$\bar{\xi}_{in} = \begin{cases} \xi_{in}/\xi_{10} & \text{balanced} \\ \xi_{in}/2\xi_{10} & \text{longitudinal} \end{cases} \quad (15)$$

Normalized Attenuation Per-Unit Length

$$\bar{\alpha} = \frac{2\pi c \xi \alpha}{R_m} = \frac{1}{2} \bar{r} \bar{c}. \quad (16)$$

In Figs. 2-5, the four dimensionless parameters \bar{c} , \bar{Z}_c , \bar{r} , and $\bar{\alpha}$ for the balanced and longitudinal modes are shown as a function of the normalized separation between the conductors b/c , with the normalized radius of the conductors a/b , as a parameter. Note that the normalizations used make the results presented in Figs. 2-7 independent of the relative permittivity ϵ_r of the material between the conductors and the conductivity σ of the conductors. The numerical values were obtained by first computing the coefficients of the surface charge density ξ_{in} using the procedure presented in [12]; the parameters of interest are readily computed from these coefficients. In all computations, the number of terms m retained in the series for the

surface charge densities (1) was taken large enough that an increase in m produced a relative change of 10^{-3} or less in the capacitances per-unit length. For example, for a separation $b/c = 0.5$ the number of terms required with the conductor size $a/b = 0.1$ was only $m = 6$, but with $a/b = 0.9$ the number of terms increased to $m = 12$. For the majority of the conductor spacings considered, the relative change was much less than 10^{-3} , typically 10^{-6} . Note that the range of allowable values for a/b at a fixed separation b/c is

$$0 < a/b < \begin{cases} 1, & 0 < b/c \leq 0.5 \\ (c/b) - 1, & 0.5 \leq b/c < 1 \end{cases}. \quad (17)$$

As expected, the capacitances for both cases shown in Fig. 2 are most sensitive to small changes in the spacing ($a/b, b/c$) when the conductors are nearly in contact, i.e., a/b near 1.0 when $b/c < 0.5$ and a/b near $(c/b) - 1$ when $b/c > 0.5$.

In Fig. 2, approximate values of the normalized capacitance per-unit length are shown as dashed lines; these were computed from the so-called "Philips" equations, (apparently given this name by C. M. Miller [8] because they originated at N. V. Philips' Gloeilampenfabrieken [19]). In normalized form these equations are, for the balanced excitation

$$\bar{c}_p = c_m/\epsilon \approx \pi/\cosh^{-1} p \quad (18)$$

where

$$p = \frac{b}{a} \frac{1 - (b/c)^2 [1 - (a/b)^2]}{1 + (b/c)^2 [1 - (a/b)^2]} \quad (19)$$

and, for the longitudinal excitation,

$$\bar{c}_p = 2c_{ge}/\epsilon \approx 4\pi/\cosh^{-1} q \quad (20)$$

where

$$q = \frac{b}{a} \frac{1 - (b/c)^4 [1 - (a/b)^2]}{4(b/c)^2}. \quad (21)$$

On examination of Fig. 2, the approximate capacitances \bar{c}_p are seen to approach the results computed from the series expansion when the spacing between the conductors is not too close, $a/b \leq 0.4$. In the limit $a/b \rightarrow 0$ (for example, see the curve $a/b = 0.1$) the agreement is very good; this is to be expected since the charged inner conductors effectively become line charges in the limit, making an approximation based on the method of images very good. In the graphs for the characteristic impedance and resistance and attenuation per-unit length for the balanced excitation, Figs. 3, 4, and 5, results obtained from approximate formulas attributed by Green *et al.* to Mead and Schelkunoff are also shown [18]. In the normalized forms the approximate formulas are

$$\bar{Z}_c = \frac{1}{\pi} \left[\ln \left(\frac{2b}{a} \frac{1 - b^2/c^2}{1 + b^2/c^2} \right) - \frac{1 + 4b^2/a^2}{16b^4/a^4} \left(1 - \frac{4b^2}{c^2} \right) \right] \quad (22)$$

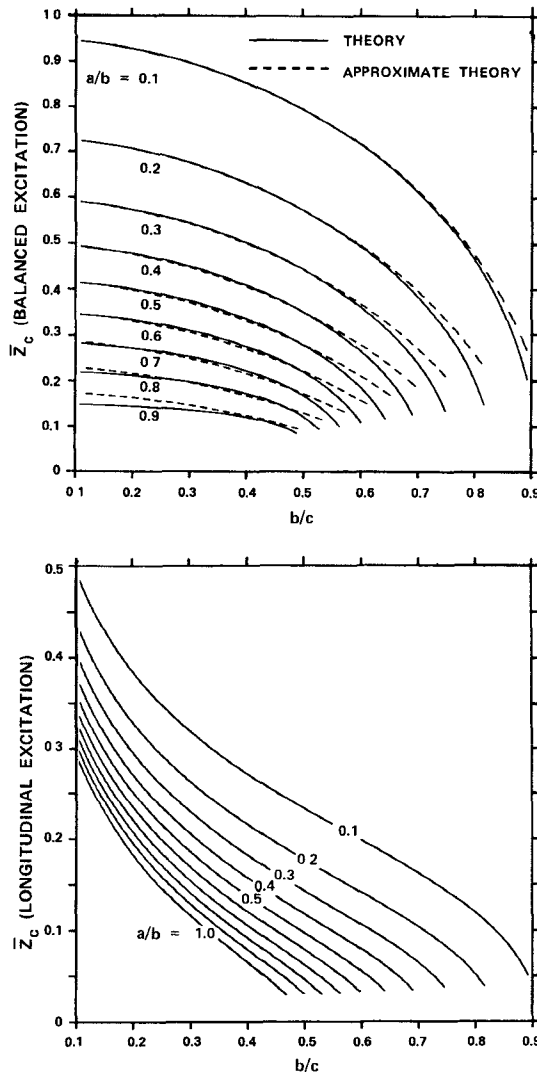


Fig. 3. Normalized characteristic impedance for balanced and longitudinal excitations versus separation of conductors with radius of conductor as parameter.

$$\bar{r} = 2 \left(\frac{c}{a} \right) \left[1 + \frac{1+2b^2/a^2}{4b^4/a^4} \left(1 - \frac{4b^2}{c^2} \right) + 8b^2/c^2 \left(1 + \frac{b^2}{c^2} - \frac{1+4b^2/a^2}{8b^4/a^4} \right) \right] \quad (23)$$

with $\bar{\alpha} = \bar{r}/2\bar{Z}_c$. These formulas are seen to be in good agreement with the numerical results computed from the series expansion when the dimensions of the conductors are not near the critical values, viz, those indicated by the inequalities (17). The proximity effect between the conductors, which is included completely in the series formulation, but not in the approximate formulas, is the cause of these differences. The useful range for the approximate formulas, of course, depends upon the amount of error that can be tolerated in a computation; but, loosely speaking, the formulas are accurate, i.e., less than 3-percent error in \bar{Z}_c , \bar{r} , and $\bar{\alpha}$, for $a/b \lesssim 0.6$ and $b/c \lesssim [0.82-1.2(a/b)]$.

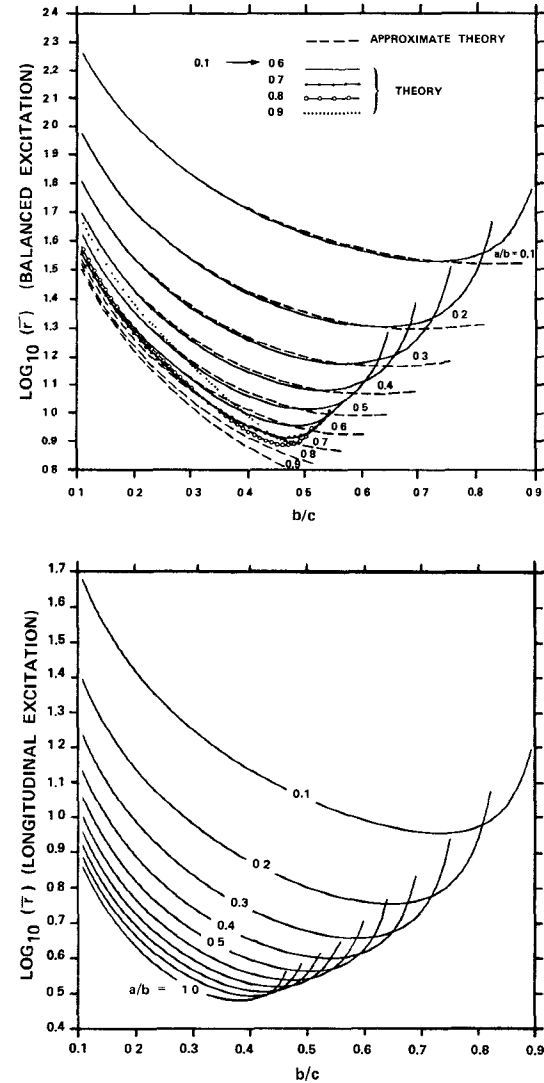


Fig. 4. Logarithm of resistance per-unit length for balanced and longitudinal excitations versus separation of conductors with radius of conductor as parameter.

The proximity effect is clearly visible in the curves for the resistance per-unit length of the line, Fig. 4. For moderate separations and conductor sizes, the resistance is seen to decrease as the radius a of the conductor is increased (fix b/c , increase a/b). This is a result of the increase in the circumference and, therefore, reduction in the resistance of the inner conductors. At larger separations and conductor sizes, increasing the radius of the conductors a can increase the resistance per-unit length, because the increase due to the proximity effect overshadows the decrease that results from the larger circumference of the conductors. The regions where this effect occurs are easily identified on the graphs as areas in which a change in the order or a crossing of the curves for constant a/b occur. For example, in Fig. 4, the ordering of the curves (a/b constant) for the balanced mode changes for values of a/b greater than 0.7. Similar behavior is observed for the curves for the attenuation per-unit length, Fig. 5.

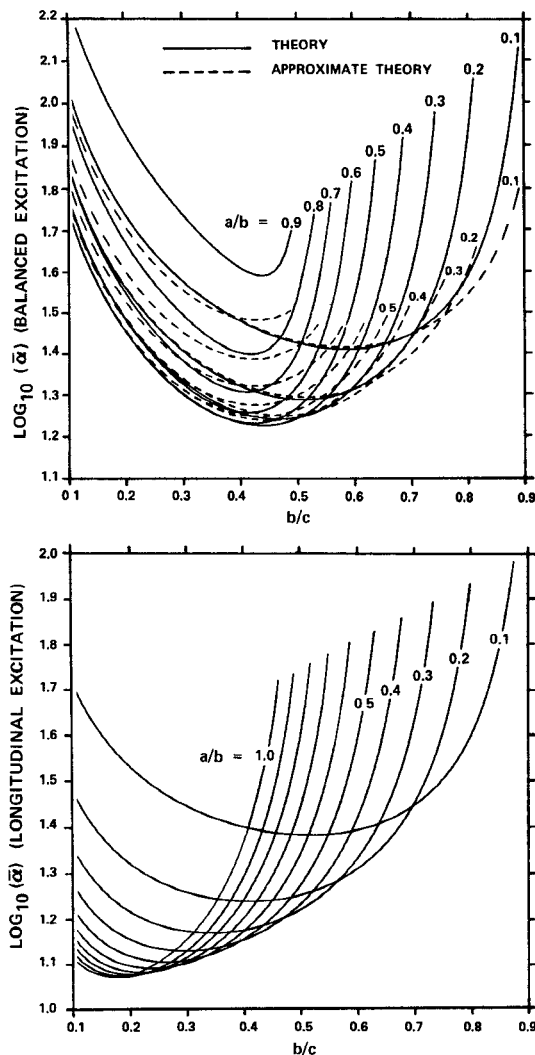


Fig. 5. Logarithm of attenuation per-unit length for balanced and longitudinal excitations versus separation of conductors with radius of conductor as parameter.

For the purpose of designing a transmission line, it is convenient to know the cross-sectional dimensions of the line that give the minimum attenuation for a specified characteristic impedance. In Figs. 6 and 7, parametric curves for the normalized impedance \bar{Z}_c and the normalized attenuation $\bar{\alpha}$ are plotted on the same graph as a function of the normalized conductor dimensions a/b and b/c for the balanced and longitudinal cases. From these graphs it is easy to determine the values of a/b and b/c that will produce a minimum value of $\bar{\alpha}$ for a fixed \bar{Z}_c . These figures also show that there are definite values of a/b and b/c that give an absolute minimum of attenuation for each method of excitation. For the balanced excitation the minimum of the normalized attenuation is $\bar{\alpha}_{\min} \approx 16.83$ when $a/b \approx 0.420$, $b/c \approx 0.436$, and for the longitudinal excitation, $\bar{\alpha}_{\min} \approx 11.75$ when $a/b \approx 1.0$, $b/c \approx 0.175$. These spacings correspond to the normalized characteristic impedance $\bar{Z}_c \approx 0.373$ for the balanced mode and $\bar{Z}_c \approx 0.214$ for the longitudinal mode. Note that the absolute minimum of $\bar{\alpha}$ for the longitudinal excitation

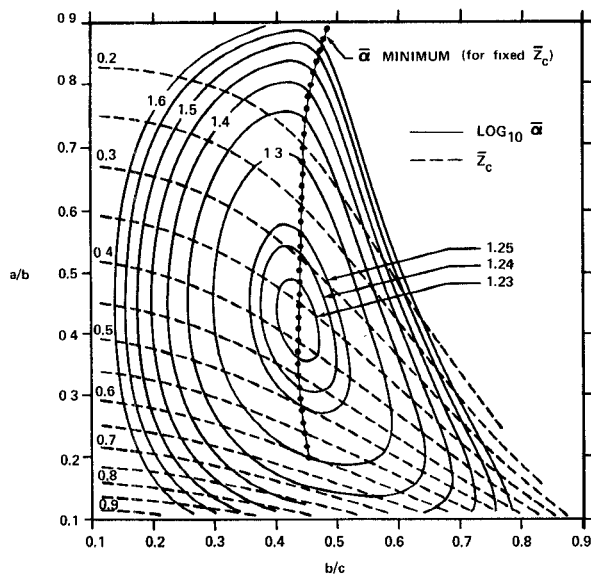


Fig. 6. Contours of constant characteristic impedance and attenuation per-unit length (balanced excitation).

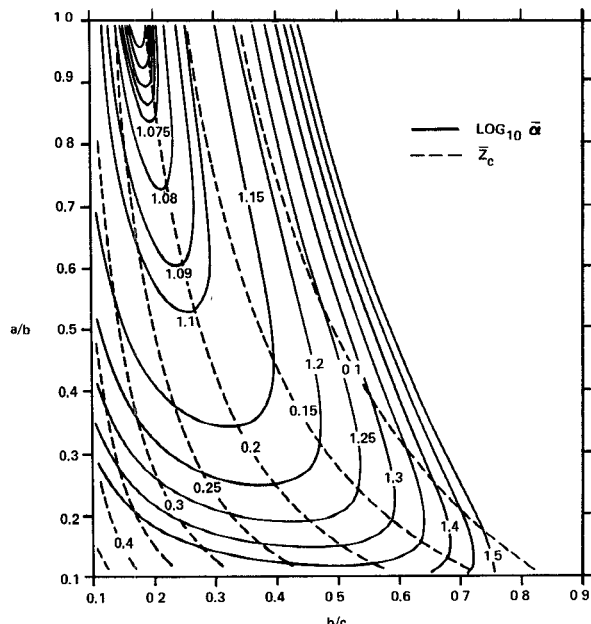


Fig. 7. Contours of constant characteristic impedance and attenuation per-unit length (longitudinal excitation).

occurs when the inner conductors of the line are touching, $a/b = 1.0$. For the longitudinal case, the surface charge (current) on the inner conductors at the point $\phi = 180^\circ$ is zero when $a/b = 1.0$, see Fig. 8; thus, the conductors coming into contact produces no drastic effects. For the balanced excitation, however, the surface charge (current) at the point $\phi = 180^\circ$ is very large for close spacings of the inner conductors and becomes infinite as they contact; this is illustrated for a spacing of $a/b = 0.95$ in Fig. 8. The different behaviors of the charge (current) near the point $\phi = 180^\circ$ for the longitudinal and balanced modes make the capacitance and resistance per-unit length for the two modes quite different for closely spaced inner conductors

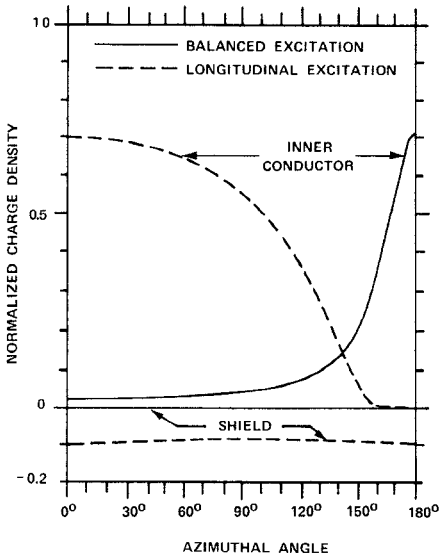


Fig. 8. Normalized charge density for balanced excitation ($b/c = 0.1$, $a/b = 0.95$) and longitudinal excitation ($b/c = 0.1$, $a/b = 1.0$).

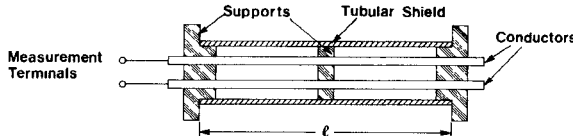


Fig. 9. Cross section of model transmission line.

(a/b near 1.0, $b/c < 0.5$). As seen in Figs. 2 and 4, the normalized capacitance \bar{c} and the normalized resistance \bar{r} per-unit length for the longitudinal mode obtain finite values in the limit $a/b \rightarrow 1.0$, whereas, both \bar{c} and \bar{r} for the balanced mode become infinite in the limit.

III. COMPARISON WITH EXPERIMENT

The capacitances c_{11} , c_{22} , and c_{ge} were measured on a model transmission line as a function of the parameters a_1/b , a_2/b , and b/c . A diagram of the experimental line is shown in Fig. 9. The perturbation introduced by the supports for the inner conductors of the line, and the fringing field that exists at the ends of the line make the electromagnetic behavior of the experimental model of length l quite different from an equal length of line in the theory, which assumes a structure that is homogeneous in the axial direction. To obtain capacitances for comparison with the theory, measurements were made on two lengths of line l_1 and l_2 . Both lengths satisfied the inequality $l \gg c$. The lines had identical support and end structures. The section of the longer line (length $l_2 - l_1$) which is not present in the shorter line has a field which is approximately uniform in the axial dimension and can be compared with the theory. The capacitances per-unit length for comparison with the theory were computed from the measurements made on the two lines; for example, for the capacitance c_{11}

$$c_{11} = \frac{C_{11}(l_2) - C_{11}(l_1)}{(l_2 - l_1)} \quad (24)$$

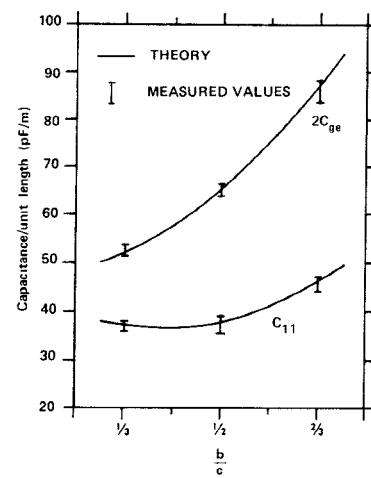


Fig. 10. Comparison of theoretical and measured values of capacitance per-unit length. (a) Line with conductors of equal radii ($a/c = 0.167$). (b) Line with conductors of unequal radii ($a_1/c = 0.167, b/c = 0.500$).

where $C_{11}(l)$ is the measured capacitance for the line of length l . This procedure for computing the capacitance essentially subtracts out the effects of the supports and the fringing at the ends.

The theoretical and measured values of the two capacitances $2c_{ge}$ and c_{11} for a symmetrical shielded pair ($a_1 = a_2$) are compared in Fig. 10(a). The capacitances are shown as a function of the ratio b/c ($a/c \approx 0.167$). The theoretical and experimental results are seen to be in good agreement. In Fig. 10(b), theoretical and measured values of the three capacitances $c_{ge1} + c_{ge2}$, c_{11} , and c_{22} for an asymmetrical shielded pair ($a_1 \neq a_2$) are shown as a function of the asymmetry a_2/a_1 ($a_1/c \approx 0.167, b/c \approx 0.500$). The theoretical and experimental results are again in good agreement. The error bars used with the experimental data in Fig. 10 include an estimate of the error associated with the instrumentation, as well as an estimate of the error that is a result of the imprecision in the size and spacing of the conductors. The latter is most critical when the conductors are at a close spacing and is the reason the size of the error bars is different for the various spacings of the conductors.

IV. CONCLUSION

The electrical parameters of the shielded-pair transmission line have been computed using the truncated harmonic expansion for the surface charge density on the conductors (1). Both the balanced and longitudinal modes of excitation were considered. For the balanced mode, the approximate formulas of S. P. Mead and S. A. Schelkunoff were shown to be accurate when proximity effects are not large, i.e., less than 3-percent error for moderate conductor sizes and spacings, $a/b \lesssim 0.6$ and $b/c \lesssim [0.82-1.2(a/b)]$. A minimum in the attenuation per-unit length of the line was found for each mode. The minimum attenuation occurs when $a/b \approx 0.420, b/c \approx 0.436$ for the balanced mode ($\bar{\alpha} \approx 16.83, \bar{Z}_c \approx 0.373$), and when $a/b \approx 1.0, b/c \approx 0.175$ for the longitudinal mode ($\bar{\alpha} \approx 11.75, \bar{Z}_c \approx 0.214$). Measured values of the capacitance per-unit length for transmission lines with inner conductors of equal and unequal radii were shown to be in good agreement with the theory.

REFERENCES

[1] M. P. Sarma and W. Janischewskyj, "Electrostatic field of a system of parallel cylindrical conductors," *IEEE Trans. Power Appar. Syst.*, vol. PAS-88, pp. 1069-1079, July 1969.

[2] P. R. Vein, "Simple series solutions of Dirichlet field problems with symmetrical circular boundaries," *Proc. Inst. Elec. Eng.*, vol. 119, pp. 1426-1428, Sept. 1972.

[3] V. Alessandrini, H. Fanchiotti, C. A. García Canal, and H. Vucetich, "Exact solution of electrostatic problem for a system of parallel conductors," *J. Appl. Phys.*, vol. 45, pp. 3649-3661, Aug. 1974.

[4] M. C. Decréton, F. E. Gardiol, and C. Maillefer, "Numerical analysis of the line capacitance and crosstalk factor for insulated wire pairs," *Archiv fur Elektronik und Übertragungstechnik*, vol. 28, pp. 415-420, 1974.

[5] K. Foster and R. Anderson, "Capacitances of the shielded-pair line," *Proc. Inst. Elec. Eng.*, vol. 119, pp. 815-820, July 1972.

[6] J. W. Craggs, "The determination of capacity for two-dimensional systems of cylindrical conductors," *Quart. J. Math. (Oxford)*, Series I, vol. 17, pp. 131-137, 1946.

[7] J. W. Craggs and C. T. Tranter, "The capacity of two-dimensional systems of conductors and dielectrics with circular boundaries," *Quart. J. Math. (Oxford)*, Series I, vol. 17, pp. 138-144, 1946.

[8] C. M. Miller, "Capacitance of a shielded balanced-pair transmission line," *Bell Syst. Tech. J.*, vol. 51, pp. 759-776, Mar. 1972.

[9] G. S. Smith, "Proximity effect in systems of parallel conductors," *J. Appl. Phys.*, vol. 43, pp. 2196-2203, May 1972.

[10] J. C. Clements, C. R. Paul, and A. T. Adams, "Computation of the capacitance matrix for systems of dielectric-coated cylindrical conductors," *IEEE Trans. Electromagn. Compat.*, vol. EMC-17, pp. 238-248, Nov. 1975.

[11] C. R. Paul and A. E. Feather, "Computation of the transmission line inductance and capacitance matrix from the quantized capacitance matrix," *IEEE Trans. Electromagn. Compat.*, vol. EMC-18, pp. 175-183, Nov. 1976.

[12] J. D. Nordgard, "The capacitance and surface charge densities of a shielded balanced pair," *IEEE Trans. Microwave Theory Tech.*, vol. MTT-24, pp. 94-10, Feb. 1976.

[13] —, "The capacitance and surface charge distributions of a shielded unbalanced pair," *IEEE Trans. Microwave Theory Tech.*, vol. MTT-25, pp. 137-140, Feb. 1977.

[14] T. A. Lenahan, "The theory of uniform cables—Part I: Calculation of propagation parameters," *Bell Syst. Tech. J.*, vol. 56, no. 4, pp. 597-610, Apr. 1977.

[15] —, "The theory of uniform cables—Part II: Calculation of charge components," *Bell Syst. Tech. J.*, vol. 56, no. 4, pp. 611-625, Apr. 1977.

[16] —, "Experimental tests of propagation-parameter calculations for shielded balanced pair cables," *Bell Syst. Tech. J.*, vol. 56, no. 4, pp. 627-636, Apr. 1977.

[17] D. V. Giri, F. M. Tesche, and S. K. Chang, "The transverse distribution of surface charge densities on multiconductor transmission lines," *IEEE Trans. Electromagn. Compat.*, vol. EMC-21, pp. 220-227, Aug. 1979.

[18] E. I. Green, F. A. Leibe, and H. E. Curtis, "The proportioning of shielded circuits for minimum high-frequency attenuation," *Bell Syst. Tech. J.*, vol. 15, pp. 248-282, 1936.

[19] J. M. van Hofweegen and K. S. Knol, "The universal adjustable transformer for U.H.F. work," *Philips Res. Rep.*, vol. 3, pp. 104-155, Apr. 1948.

[20] A. W. Gent, "Capacitances of shielded balanced-pair transmission lines," *Elect. Commun.*, vol. 33, pp. 234-240, Sept. 1956.

[21] R. Plonsey and R. E. Collin, *Principles and Applications of Electromagnetic Fields*. New York: McGraw-Hill, 1961, pp. 96-101.